ELSEVIER

Diamond and Related Materials 7 (1998) 233–237

DIAMOND AND RELATED MATERIALS

Use of different excitation wavelengths for the analysis of CVD diamond by laser Raman spectroscopy

S.M. Leeds [a,*], T.J. Davis [b], P.W. May [a], C.D.O. Pickard [b], M.N.R. Ashfold [a]

[a] *School of Chemistry, University of Bristol, Cantock's Close, Bristol, BS8 1TS, UK*
[b] *H.H. Wills Physics Laboratory, Tyndall Avenue, Bristol, BS8 1TL, UK*

Received 23 June 1997; accepted 9 September 1997

Abstract

Raman spectroscopy has been shown to be an accurate technique for the qualitative characterisation of chemical vapour deposited (CVD) diamond films. The intensities of the diamond and non-diamond components in the spectrum vary with the wavelength of the laser excitation. This shows that laser Raman at different wavelengths can be used as a selective probe for the different constituents of the deposited film.

In the present work, this selectivity has been used to examine the effect of methane concentration during growth on the Raman spectra of CVD diamond. Diamond films were deposited on single crystal Si(100) wafer substrates by microwave plasma enhanced, and hot filament assisted CVD. Methane concentrations of 0.36–2.16% in hydrogen were used as the feedstock. Laser wavelengths ranging from the ultraviolet (244 nm) to the infra-red (780 nm) were used to perform Raman spectroscopy on the deposited diamond films. Scanning electron microscopy (SEM) was used to determine the morphology of the films and related to the Raman spectra. © 1998 Elsevier Science S.A.

Keywords: Chemical vapour deposition: Raman spectroscopy; Laser excitation

1. Introduction

Diamond films can be deposited from the gas phase by a variety of CVD techniques, each having its own advantages and disadvantages [1]. In this study, we have chosen to examine films grown by two of the most popular methods: hot filament assisted CVD (HFCVD), and microwave plasma enhanced CVD (MPCVD) [1,2].

Paralleling the diversity of deposition methods, a wide range of analytical techniques have been used to study CVD diamond films. Laser Raman spectroscopy, in particular, has become an important technique for the analysis of diamond [3–6]. The first-order diamond Raman peak at *ca.* 1333 cm^{-1}, due to single phonon scattering, is unambiguous evidence for the presence of diamond in a deposited film. However, the existence of non-diamond carbon components in CVD diamond produces several overlapping peaks in the same wavenumber region as the first order diamond peak. The intensities of these features are dependent on the deposition conditions, and may be due to graphitic [7–9], or amorphous carbon components in the film [8,9]. This, combined with the larger Raman cross-section of the graphite component relative to the diamond (~50 times) [10], and that of the amorphous component relative to diamond (~233 times) [11], complicates the interpretation of spectra in terms of diamond film quality. In addition, the intensities and peak positions of some non-diamond carbon peaks have been shown to be dependent on the wavelength of the laser excitation used to obtain the spectra [12–16]. This has been ascribed to resonance effects [9,14], or to an increased absorption of the laser radiation by non-diamond components of the film with decreasing wavelength [12,16].

It is the aim of the present work to relate features of CVD diamond Raman spectra to the inlet chemical composition for methane/hydrogen gas mixtures, over a wide range of laser excitation wavelengths, for HFCVD and MPCVD.

2. Experimental details

Continuous diamond films were deposited on Si (100) wafer substrates (of area 1–3 cm^2) by microwave plasma,

* Corresponding author. Fax: +44 117 925 1295; e-mail: stuart.leeds@bris.ac.uk

PII S0925-9635(97)00261-6

and hot filament CVD. Substrates were manually abraded with 1–3-μm diamond grit as a nucleation enhancing pre-treatment. HFCVD and MPCVD were carried out on samples using methane/hydrogen gas mixtures, with methane concentrations of 0.36–2.16% as feedstock gases.

MPCVD was carried out using an ASTeX 2.45-GHz, 1.5-kW microwave generator coupled to a custom built reaction chamber. The plasma was not in contact with the reactor walls, and its lower visible edge was ~4 mm above the substrate surface. The substrate was heated resistively (in addition to plasma heating) by a serpentine graphite element contained in the molybdenum substrate holder (145 mm in diameter). A thermocouple was used to measure the local temperature in the substrate holder. A thermocouple reading of 800 °C was maintained during all depositions. The actual substrate temperature was estimated to be ~1000 °C. HFCVD was carried out in a standard CVD reactor, using a 0.25-mm-diameter, six-turn tantalum filament approximately 1 cm long. The filament was located ~4 mm above the substrate surface. Growth conditions used for both methods are listed in Table 1.

Raman spectra were taken from the centre of the as grown samples using a number of different laser excitation wavelengths. Infra-red excitation was carried out using the 780-nm (1.59 eV photon energy) output of a HeCd laser. Studies in the visible region were made using the 633-nm line (1.96 eV) of a HeNe laser and the 514-nm line (2.41 eV) of an argon ion laser. Ultraviolet radiation was obtained at 244 nm (5.09 eV) by frequency-doubling the 488-nm line of an argon ion laser. The samples were analysed at 300 K, in a back-scattering geometry, in all cases. All of the Raman data acquisition and processing were done using Renishaw confocal imaging systems.

The films were also studied by SEM to determine their thickness and microstructural characteristics.

Table 1
Growth conditions used for sample preparation by microwave plasma and hot filament CVD

Growth conditions	MPCVD	HFCVD
Pressure (Torr)	30	20
Total gas flow (sccm)	200	200
Substrate temperature (°C)	900	900
Deposition time (h)	6	6.75
Microwave power (W)	1000	
Filament temperature (°C)		2400
Methane concentration (%)	0.36 (Sample A)	0.36 (Sample F)
	0.72 (Sample B)	0.72 (Sample G)
	1.08 (Sample C)	
	1.44 (Sample D)	
	2.16 (Sample E)	2.16 (Sample H)

3. Results

The growth rates and morphology of the diamond films grown at different methane concentrations, deduced by SEM, compare well with those presented by other authors [17,18]. The films were all 1–4 μm thick. The best crystallite quality, as judged by the size and smoothness of facets, occurred for a methane concentration of 0.72%. Above this concentration, crystallites became smaller until a smooth nanocrystalline film was formed for growth at 2.16% methane concentration.

Raman spectra of samples A–E (MPCVD), taken using a wide range of laser wavelengths, are presented in Fig. 1a–d. All spectra, except the infra-red, have been normalised to have equally intense diamond Raman peaks and offset for clarity.

3.1. Infra-red Raman spectra

The infra-red spectra were not normalised as the diamond peak was either very small or non-existent for this wavelength of excitation. In some of the spectra, particularly those grown with a low methane concentration, there are a number of well-defined peaks. The number, position, and intensity of these peaks change in a random manner for different positions on the film. Broad bands around 1300 cm^{-1} and 1570 cm^{-1} are evident in the spectra. These bands become more pronounced as the methane concentration increases. A weak, broad band appears as a shoulder at ~1160 cm^{-1} for a methane concentration of 1.44%. This feature becomes more intense as the methane concentration is increased.

3.2. Red Raman spectra

The spectra excited at 633 nm show a discernible diamond Raman line at all methane concentrations. The most intense diamond peak was found for the 0.72% methane concentration sample, consistent with the SEM evidence regarding crystallite quality. The intensity of the non-diamond carbon bands increases with increasing methane concentration. Again, the shoulder band seen in the infra-red spectra is present in these films, except that its position has shifted to 1100 cm^{-1}.

3.3. Green Raman spectra

The spectra obtained using 514 nm light show weaker non-diamond carbon features than the 633 nm spectra. The diamond line is easily discernible, and the spectrum is superimposed on an intense photoluminescence (PL) background. The shoulder noted previously has developed into a pronounced peak at ~1140 cm^{-1} for the films grown with a higher methane concentration.

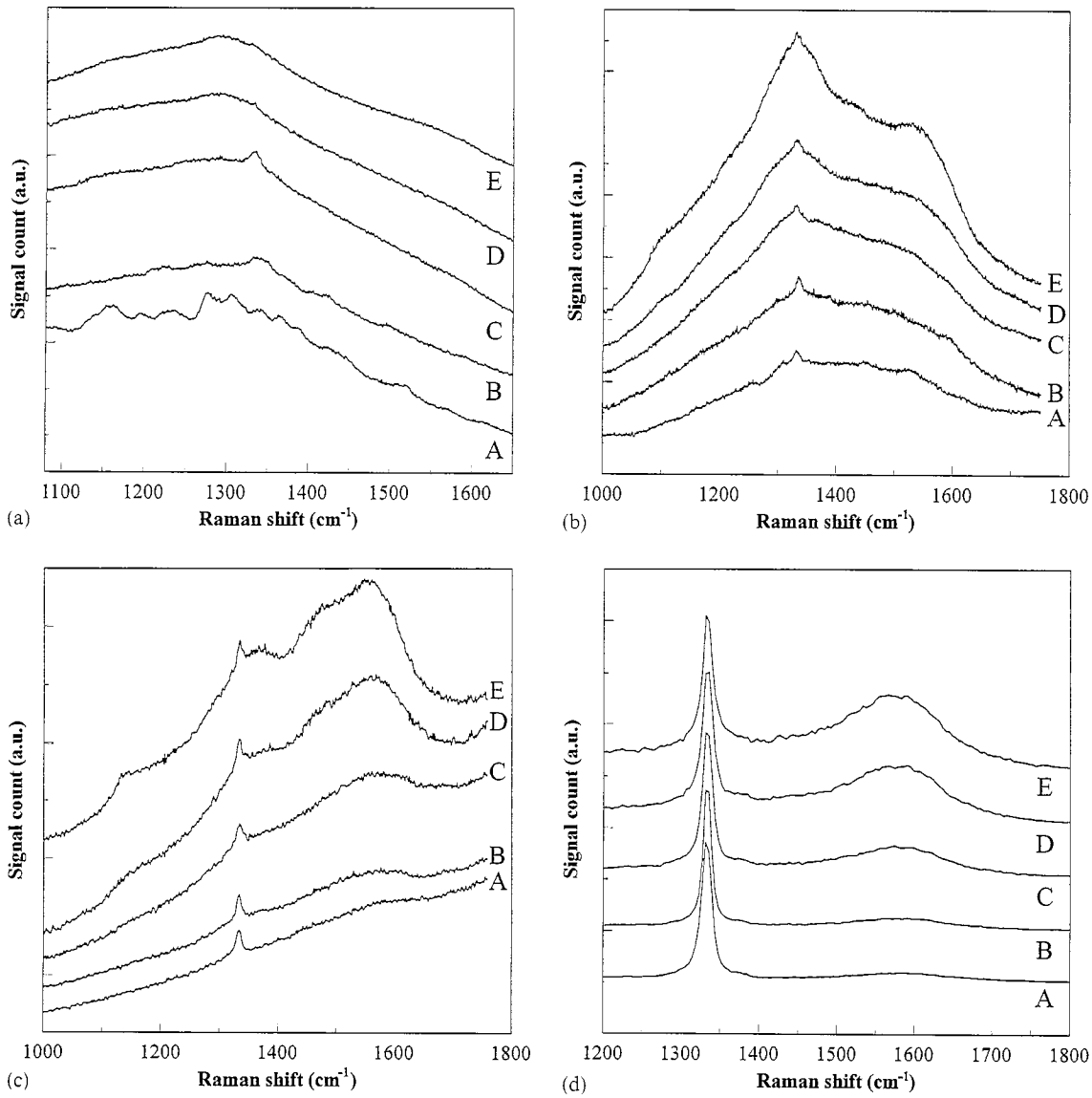

Fig. 1. Raman spectra of samples A–E (see Table 1 for deposition conditions). (a) Spectra taken in the IR at 780 nm. (b) Raman spectra of the same samples excited with visible (red) light at 633 nm. (c) Raman spectra excited at 514 nm. (d) Raman spectra taken in the UV at 244 nm. Spectra (b)–(d) have been normalised to have the same diamond peak intensity and offset on the vertical axis for clarity and hence are plotted in arbitrary units (a.u.).

3.4. Ultraviolet Raman spectra

Spectra obtained in the UV are dominated by the diamond Raman line. Non-diamond carbon features appear as a broad band at $\sim 1570\ cm^{-1}$, the relative intensity of which increases as the methane concentration is increased.

3.5. HFCVD films

Spectra obtained from the films grown using the HFCVD system showed very similar trends to the ones from the MPCVD system, and so these spectra have not been shown for brevity. However, this does highlight the fact that laser Raman is a reliable diagnostic for CVD diamond films, independent of deposition technique.

4. Discussion

We have shown that the spectra obtained from laser Raman spectroscopy are very sensitive to the wavelength of the excitation source. This has previously been shown by other authors [12–16], but not in a series of samples grown under identical conditions with a systematic variation of methane concentration. Our results show a number of trends. Perhaps the most striking of these is that the relative sensitivity of the technique to the D-band and G-band (i.e. the disordered and ordered

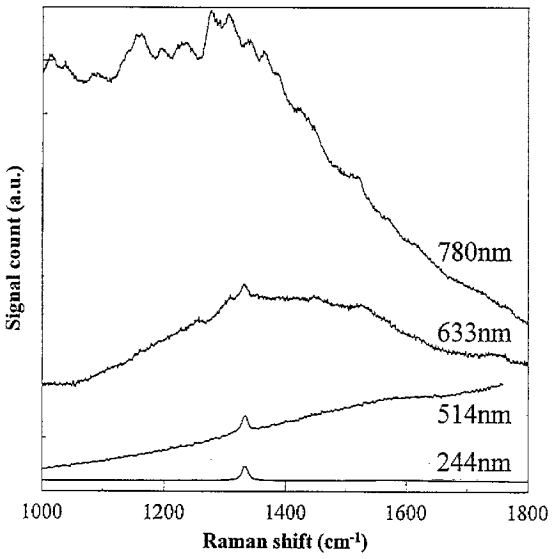

Fig. 2. Raman spectra taken using four different laser excitation wavelengths for 0.36% methane concentration. The spectra have been normalised to the heights of the diamond peak. Curve-fitting these spectra allows the ratio of the diamond peak to G-band areas to be calculated. Values for these ratios are: 2:1, 1:6, 1:25 and ~1:50, respectively, for increasing laser wavelengths. Note also the shape of the underlying PL background in each case. For the IR spectrum, the intense PL peak is to the left of the Raman region. The 633-nm Raman spectrum sits on top of the photoluminescence peak, whereas the 514 nm Raman spectrum sits on the other side of the photoluminescence peak to the IR spectrum. The UV Raman spectrum exists even further from the PL peak, which scarcely contributes to the signal, giving a flat background.

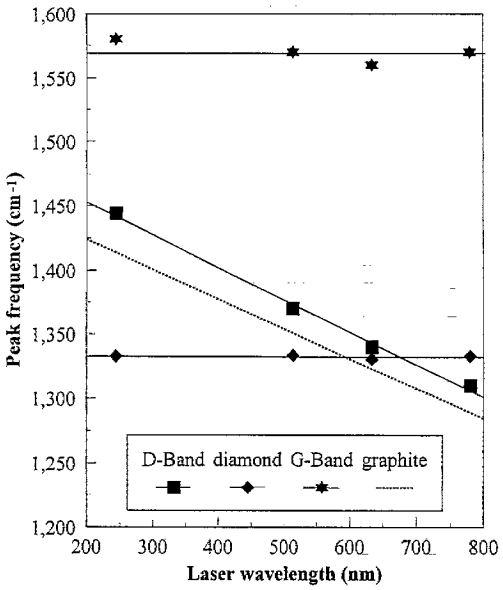

Fig. 3. Graph showing the positions of the major peaks in the Raman spectrum as a function of laser wavelength. The peaks shown are the diamond peak at ~1332 cm^{-1}, the graphite G-band centred ~1580 cm^{-1}, and the graphite D-band whose position varies over the range 1450–1300 cm^{-1}. Also shown as a dashed line is the trend from Kawashima and Katagiri [21] for microcrystalline graphite.

graphite region, respectively) decreases with decreasing wavelength. This can be seen in Fig. 2, where the ratios of the diamond peak to graphite band change from 2:1 to ~1:50 as we move from UV to IR excitation. This means that for UV Raman, the diamond peak is very prominent, and therefore little information about non-diamond species can be gathered. Conversely, for red and IR Raman, the diamond peak is often obscured by the large signal from non-diamond carbon.

Previous authors have ascribed this enhancement of the diamond signal at a lower wavelength to either an absorption effect [12,16] or a resonance effect [9,14]. The absorption effect is due to the differing absorption depth of graphite, and therefore differing interaction volume, at different laser wavelengths, causing a change in the signal intensity. Alternatively, the resonance model explains the change as a proximity of the incident laser wavelength to electronic transitions in non-diamond material. In the case of IR Raman, the large number of peaks in the 1200–1600 cm^{-1} region may be an indication of resonance phenomena. A detailed investigation of which of these two models best explains these data will be published in a future paper (private communication).

Other trends seen in Fig. 1a–d are that when using the green, red or IR laser, a shoulder in the spectrum appears containing a peak around 1100–1160 cm^{-1}, which has been attributed to amorphic or nanocrystalline diamond [19]. Note that this peak was not seen in the UV spectra. We do not at present have an explanation for this observation.

Fig. 3 shows that the position of the G-band and the diamond peak remain constant with increasing laser wavelength, whereas the D-band shifts down in frequency. This behaviour has been observed in microcrystalline graphite [20] and DLC films [21], but has not yet been satisfactorily explained. Fig. 3 also shows the trend line from [20] for microcrystalline graphite, and since our data agree with this within the range of experimental error, we can say that the inclusions in our CVD films can be best explained as microcrystalline graphite, rather than another form of non-diamond carbon. This also agrees with the observation of the G-band occurring at 1580 cm^{-1}, rather than at around 1450 cm^{-1} which would indicate amorphous carbon.

If we assume that the non-diamond component of the films behaves similarly to microcrystalline graphite, then it would be possible to use the known Raman cross-sections of diamond and graphite to obtain more accurate estimates of the sp^2:sp^3 ratios. Studies of this will appear in a future publication.

Care must be exercised, however, in obtaining quantitative results for the ratios of peak intensities, since as the wavelength increases, the Raman spectrum overlaps different regions of the photoluminescence background (as demonstrated in Fig. 2). This luminescence spectrum is complex and requires careful fitting and deconvolution (for example, by using two comparatively closely spaced

wavelengths, e.g. 488 and 514 nm), but this will be necessary to obtain meaningful values for the graphite-to-diamond ratios.

5. Conclusions

We have shown that care must be taken when interpreting laser Raman data, since the ratios of peak areas, some peak positions, and the photoluminescence background are all highly dependent upon the choice of laser wavelength. However, by combining spectra taken over a range of wavelengths, much more information can be gained about the components of the films than can be obtained from using one wavelength alone. However, the fundamental theories for explaining all of these effects are at an early stage of development. Therefore, attempts need to be made to unite these preliminary observations with an accurate model.

Acknowledgement

We would like to thank the Engineering and Physical Sciences Research Council for project funding. PWM would like to thank the Royal Society for financial support. TJD would like to thank Renishaw Transducers for funding. We would also like to thank Renishaw Transducers, and the University of Bristol Interface Analysis Centre for the use of infra-red and red Raman spectrometers respectively, and the University of Leeds for the ultraviolet measurements.

References

[1] P.K. Bachmann, W. van Enckevort, Diamond Relat. Mater. 1 (1992) 1021.
[2] M.N.R. Ashfold, P.W. May, C.A. Rego, N.M. Everitt, Chem. Soc. Rev. 23 (1994) 21.
[3] D.S. Knight, W.B. White, J. Mater. Res. 4 (1989) 385.
[4] W.A. Yarbrough, R. Messier, Science 247 (1990) 688.
[5] L.H. Robins, E.N. Farabaugh, A. Feldman, J. Mater. Res. 5 (1990) 2456.
[6] I.P. Hayward, K.J. Baldwin, D.M. Hunter, D.N. Batchelder, G.D. Pitt, Diamond. Relat. Mater. 4 (1995) 617.
[7] W. Zhu, C.A. Randall, A.R. Badzian, R. Messier, J. Vac. Sci. Technol. A 7 (1989) 2315.
[8] R.J. Nemanich, J.T. Glass, G. Lucovsky, R.E. Shroder, J. Vac. Sci. Technol. A 6 (1988) 1783.
[9] L. Fayette, B. Marcus, M. Mermoux, L. Abello, G. Lucazeau, Diamond Relat. Mater. 3 (1994) 438.
[10] N. Wada, S.A. Solin, Physica B 105 (1981) 353.
[11] S.R. Sails, D.J. Gardiner, M. Bowden, J. Savage, D. Rodway, Diamond Relat. Mater. 5 (1996) 589.
[12] J. Wagner, M. Ramsteiner, Ch. Wild, P. Koidl, Phys. Rev. B 40 (1989) 1817.
[13] M. Yoshikawa, G. Katagiri, H. Ishida, A. Ishitani, M. Ono, K. Matsumura, Appl. Phys. Lett. 55 (1989) 2608.
[14] J. Wagner, C. Wild, P. Koidl, Appl. Phys. Lett. 59 (1991) 779.
[15] J. Wagner, C. Wild, W. Müller-Sebert, P. Koidl, Appl. Phys. Lett. 61 (1992) 1284.
[16] C.D. Clark, C.B. Dickerson, J. Phys. D 4 (1992) 869.
[17] A.M. Bonnot, Phys. Rev. B 41 (1990) 6040.
[18] K. Kobashi, K. Nishimura, Y. Kawate, T. Horiuchi, Phys. Rev. B 38 (1988) 4067.
[19] A.M. Nistor, J. Van Landuyt, V.G. Ralchenko, E.D. Obratsova, A.A. Smolin, Diamond Relat. Mater. 6 (1997) 159.
[20] Y. Kawashima, G. Katagiri, Phys. Rev. B 52 (1995) 10053.
[21] M. Yoshikawa, G. Katagiri, H. Ishida, A. Ishitani, Solid State Commun. 66 (1988) 1177.